

# Velocity distributions in clusters of galaxies

Andreas Faltenbacher and Juerg Diem and

UCO /Lick Observatory, University of California at Santa Cruz, 1156 High Street, Santa Cruz, CA 95064, USA

7 February 2020

## A B S T R A C T

We demonstrate, using a dissipationless N-body simulation of a galaxy cluster, that the velocity dispersion of subhalos depends strongly on the selection criterion: Applying a lower limit on the present bound mass of subhalos leads to higher velocity dispersions for the subhalos compared to the diffuse dark matter (positive velocity bias). Hardly any bias is detected if subhalos are required to exceed a minimum mass before accretion onto the host. It has been shown, that the latter criterion results in subhalo samples that closely resemble the spatial distribution of observed galaxy clusters, therefore it subsequently is referred to as galaxy sample. The velocity distributions of both, the galaxy sample and the diffuse dark matter follow Maxwell distributions with very similar temperatures. The velocity dispersion of the diffuse dark matter is translated into a temperature profile of the intra cluster gas (ICM) which is in good agreement with recent X-ray observations. From the temperature the adiabatic sound speed can be derived. A comparison of this sound speed with the velocities of galaxies results in an average Mach number of 1.24. 65% of the galaxies move supersonically and 8% have Mach numbers larger than 2.

**Key words:** cosmology:theory { galaxies:clusters,velocity distribution { methods: numerical

## 1 INTRODUCTION

Spectroscopic measurements of the velocity distributions in groups and clusters of galaxies have extensively been used to investigate their dynamical states. It is commonly agreed that line of sight distributions similar to Gaussian reveal relaxed systems (e.g. Chincarini & Rood 1971, 1977; Halliday et al. 2004; Lokas et al. 2005). Non-gaussianity is usually associated with merging or even multiple-merging events (e.g. Colless & Dunn 1996; Cortees et al. 2004; Adami et al. 2005; Girardi et al. 2005). Apart from major merging events, also a selection which favours recently accreted galaxies may cause non-gaussianity. For instance, Caldwell (1987) find that the velocity distribution of star-forming galaxies of the Fornax cluster is non-Gaussian, whereas that for the E/S0 galaxies is Gaussian. And Mendes de Oliveira et al. (2006) show that the exclusion of the emission-line galaxies, which are believed to be recently accreted by cluster RX J1552.2+2013, generates a distribution more similar to Gaussian.

The high resolution imaging of the X-ray observatories XMM-Newton and Chandra provide complementary means to study the dynamical state of groups and clusters of galaxies (e.g. Kempner & David 2004; Neumann et al. 2001, 2003). The studies of Vikhlinin et al. (2001); Yamasaki et al. (2002); Sun et al. (2005) have shown that massive galaxies ( $> L^*$ ) can retain their X-ray corona,

even in very dense environment. The interaction of these cool gas cores of the galaxies with the hot intra cluster medium (ICM) makes it possible to measure the velocities of the galaxies with respect to the ambient cluster gas. An investigation by Machacek et al. (2005) of the motion of NGC 1404 in the Fornax cluster implies near sonic motion (Mach number 0.83–1.03) with a velocity  $531 - 657 \text{ km s}^{-1}$  relative to the surrounding cluster gas. Sun et al. (2005) find bow shock pattern ahead of an infalling galaxy. The sharp asymmetry of their X-ray corona is interpreted as the result of ram pressure and results in an estimated Mach number of 2.4–4.2. Also Machacek et al. (2005) finds a spiral galaxy in the Pavo Group moving with Mach numbers in the range between 2–4.

Cold dark matter (CDM) simulations have revealed an excess velocity dispersion of subhalos compared to the velocity dispersion of diffuse dark matter within the host halo (Ghigna et al. 2000; Colin et al. 2000; Diemand et al. 2004). In other words, the subhalo population shows a positive velocity bias or is hotter in comparison with the diffuse component. This raises the question, whether cluster galaxies also move faster than the dark matter background, because it would affect dynamical cluster mass estimates (e.g. Lokas et al. 2005). Furthermore, it is tempting to explain supersonic motions recently found in X-ray observations simply by the positive velocity bias. However, as we

## 2 Faltenbacher and Diem and

discuss below, the strength of the velocity bias crucially depends on the method of the subhalo selection. We will focus on two different approaches. On the one hand we will consider all bound substructures above a certain mass limit at present. If these subhalos are assumed to host galaxies the spatial distribution of cluster galaxies would be much more extended than the dark matter and not in agreement with observations (Diem and et al. 2004). On the other hand we will select only those subhalos, which have exceeded a certain mass limit before accretion onto the host. This approach is justified by the assumption that the amount of star formation within a halo is connected to the depth of its potential during the epoch when the gas is accreted, i.e. to its mass before entering the group or cluster. Using this accretion time subhalo selection criterion Nagai & Kravtsov (2005) were successful in matching the distribution of observed cluster galaxies with the results of N-body simulations. Semi-analytic modeling of galaxy formation combined with high resolution dissipationless galaxy cluster simulations (Springel et al. 2001; Gao et al. 2004) also produces to galaxy cluster with similar spatial and velocity distributions for the dark matter and the galaxies. This is probably because similar halos were populated with galaxies as in Nagai & Kravtsov (2005) but in a less transparent, more model dependent way. Similar spatial distributions of galaxies and dark matter were also found in hydrodynamic cosmological simulations (see Nagai & Kravtsov 2005; Sommer-Larsen et al. 2005; Maccio' et al. 2005). Additionally they include the dynamical effect of dense baryonic cores (galaxies) inside subhalos which helps them to survive even in very dense environments (within about 0.1 of virial radius of the host halo) where most pure dark matter subhalos are stripped below the resolution limit of current simulations. We will exclude this very inner region where the baryonic component becomes essential for survival from our analysis since we are using a pure dark matter cluster simulation.

The spatial distribution of tracers in cosmological dark matter halos is related to their velocity distribution to a very good approximation via the spherical, stationary Jeans equation (Diem and et al. 2004, 2005): A spatially extended component (like subhalos) is hotter than the dark matter whereas more concentrated subsets (like intracluster light or globular clusters) are colder (and on more radial orbits, see Diem and et al. 2005). Since cluster galaxies tend to trace the mass distribution one expects little or no difference between galaxy and dark matter velocity distribution. Clusters of galaxies are formed by gravitational collapse which results in a Maxwell velocity distribution for the diffuse component. Even if the diffuse component and the galaxies have equal temperatures, a large fraction of galaxies move supersonically, because of the high velocity tail of the Maxwell distribution. In x2 the simulation and the two subhalo samples are described. x3 discusses the impact of the selection criterion of the subhalo samples on the velocity dispersions. In x4 the average Maxwell numbers of galaxies in clusters are computed assuming a Maxwell distribution for the galaxies and the diffuse background. In x5 the results are summarized.

## 2 SIMULATION AND SUBHALO SAMPLES

We analyse a cluster-sized dark matter halo generated within a cosmological N-body simulation ( $m = 0.268$ ,  $= 0.7$ ,  $s = 0.7$ ,  $h_{100} = 0.71$ ). The peak mass resolution of this simulation is  $2.2 \cdot 10^7 M_\odot$  with a softening length of 1.8 kpc. The cluster has a virial mass of  $3.1 \cdot 10^{14} M_\odot$  at  $z = 0$  which corresponds to  $14 \cdot 10^6$  particles within the virial radius<sup>1</sup>. This cluster was named D12 in Diem and et al. (2004).

We apply two different recipes to create the subhalo samples. On the one hand we use SKID<sup>2</sup> with a linking length of 5 kpc and identify all bound structures comprising at least 10 particles as subhalos. That way we find 4239 subhalos within the virial radius of the cluster at  $z = 0$ . Subsequently this subhalo sample will be called sample a. On the other hand we trace back the most bound particle of the subhalos, which were identified by SKID in the same manner as mentioned above and compare their positions with those of old halos which are found with FOF in earlier outputs using a linking length of 0.2 times the mean particle separation. The final sample encompasses only those subhalos, which had progenitors (FOF old halos) containing a minimum of  $200 (4.4 \cdot 10^9 M_\odot)$  particles at least once during their old-halo phase. In total, 367 subhalos meet this criterion. These subhalos are assumed to host galaxies. This approach was used by Nagai & Kravtsov (2005) to assign galaxies (luminous baryonic matter) to subhalos derived from pure dark matter N-body simulations. Subsequently we will call this sample galaxy-sample or synonymously sample b. Since we have only ten outputs the time between them is quite large, about 1.3 Gyr. This means that we fail to select some halos which are above the minimum mass only for a short time before they are accreted onto a larger host system. With many more outputs one would be able to determine the maximum mass of a subhalo just before accretion more accurately and one presumably would find some more halos with large enough progenitors. We assume that this inaccuracy does not affect our results.

Figure 1 displays the cumulative radial number distribution for the different samples and the diffuse dark matter component. As centre the most bound particle is chosen, which is assumed to coincide with the central brightest galaxy of observed clusters. We start the cumulation for all components, subhalos, galaxies and diffuse dark matter, at 20% of the virial radius ( $0.2r_{\text{vir}}$ ). The inner 20% are excluded, because the high density environment is likely prone to artificial loss of substructure due to numerical overcooling. Additionally the survival of galaxies in this very inner region starts to depend on the mass distribution within their inner, baryon dominated parts (Nagai & Kravtsov 2005; Maccio' et al. 2005). The galaxy sample (sample b, solid line) and the diffuse dark matter profile (dashed line) are very similar, whereas the halos of sample a (dotted line) show a definite deviation. The selection criterion based on the current mass of the subhalos ignores the history of the individual subhalos. Thus a freshly accreted low mass halo and tidally stripped old (i.e. early accreted) subhalo are treated

<sup>1</sup> According to the definition used here the virial radius encloses 368 times the mean matter density.

<sup>2</sup> <http://www-hpcc.astro.washington.edu/tools/skid.htm>

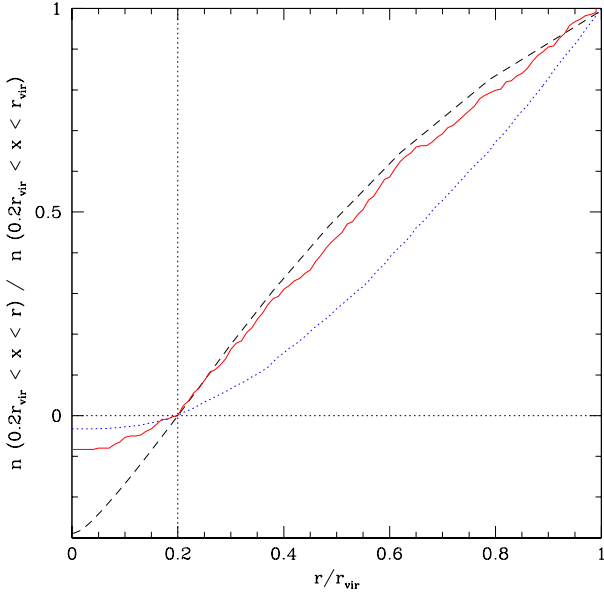


Figure 1. Normalised radial number distribution for the total amount of dark matter (dashed line) and halos belonging to the two different sub-samples a and b displayed in dotted and solid lines, respectively. The region within  $0.2r_{vir}$  is excluded from accumulation to reduce the influence of numerical overmerging.

equivalently. Due to the steep mass function of old halos most systems ever accreted had masses not much larger than the median mass. Those who still lie above this median mass today (like our sample a) are mostly systems which have lost little mass, i.e. recently accreted halos in the outer part of the cluster (see Kravtsov et al. 2004; Zentner et al. 2005). The selection criterion for the 'galaxies' (sample b) ensures that only subhalos with a substantial initial mass (200 particles) are counted as members of the sample. Since these halos must have retained at least 10 particles to be found by the SKID halo finder at  $z = 0$ , they can loose 95% of their initial mass on their orbits within the cluster potential well (even more if they were more massive at the moment of accretion). The subhalos of the galaxy sample are quite persistent. In that respect the galaxy sample is very similar to the diffuse dark matter component, because by definition the building blocks of the diffuse component (the simulation particles) are indestructible.

### 3 DEPENDENCE OF THE VELOCITY DISTRIBUTION ON THE SUBHALO SELECTION

Figure 2 displays the normalised ( $v_{c,max} = 958 \text{ km s}^{-1}$ ), radially binned velocity dispersions of the samples a and b with open and filled symbols, respectively. The dotted vertical line marks the exclusion area, the velocities of subhalos residing inside  $0.2r_{vir}$  will not be considered in the further analysis, because subhalo survival in this area is likely to be affected by numerical overmerging and the missing baryonic component. For a fair comparison we also exclude the velocity contribution of the diffuse dark matter within that radius. All velocities are computed relative to the centre of

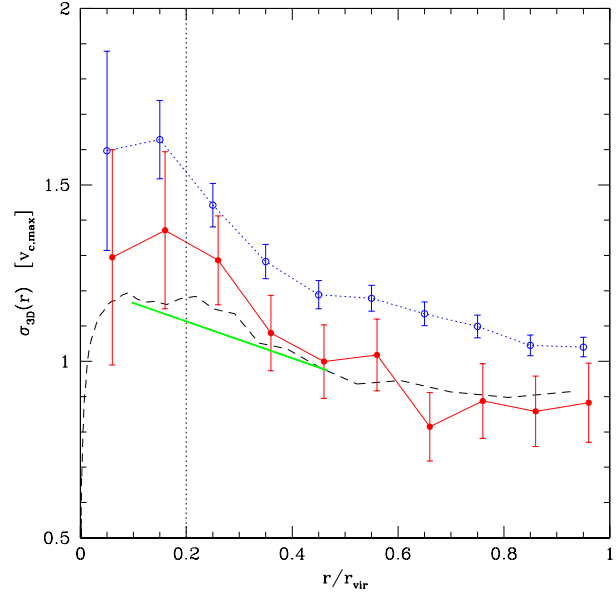


Figure 2. Normalised velocity dispersion profiles ( $v_{c,max} = 958 \text{ km s}^{-1}$ ) for all dark matter particles (dashed line) and halos belonging to the sub-samples a and b displayed in dotted and solid lines, respectively. The error bars display the 1  $\sigma$  deviations. The region within  $0.2r_{vir}$  is excluded from the further analysis due to the appearance of numerical overmerging. The solid line ranging from 0.1 to 0.47 times the virial radius is the velocity dispersion equivalent to the X-ray temperatures for a cluster of this size, see x4.

mass velocity ( $v_{COM}$ ), i.e. the average velocity of all particles within  $r_{vir}$ . For completeness it should be mentioned here, that the spatial distance between the most bound particle and the centre of mass ( $COM$ ) is  $0.053r_{vir}$  and the velocity difference between the most bound particle and  $v_{COM}$  equals  $0.04v_{c,max}$ . The solid line ranging from  $0.1r_{vir}$  to

$0.45r_{vir}$  shows the velocity dispersion derived from X-ray temperature profiles for clusters with comparable size (see x4). The dispersion of the diffuse dark matter component is shown as dashed line. For all radii the velocity dispersion of sample a deviates by more than 15% from the diffuse component. The difference between these two distributions increases towards the centre, approaching values as large as 30% at  $0.2r_{vir}$ . There also appears to be a slight deviation of the velocity dispersion of sample b compared to the diffuse component, however, this deviation hardly exceeds the 1  $\sigma$  uncertainty levels. The velocity dispersion profile of the galaxy sample (sample b) and the diffuse dark matter component are very similar.

As discussed before, the similarity of the galaxy sample and the diffuse component in the density profiles results from the comparable persistence of the sample members. Therefore it is reasonable to consider the galaxy sample as a set of indestructible particles similar to the simulation particles, but with different masses. Due to energy conservation (and without including dynamical friction or other energy redistributing mechanisms) the gravitational collapse of a distribution of different mass particles leads to equal velocity dispersions within different mass bins. Therefore one expects no spatial and no velocity bias between the galaxy

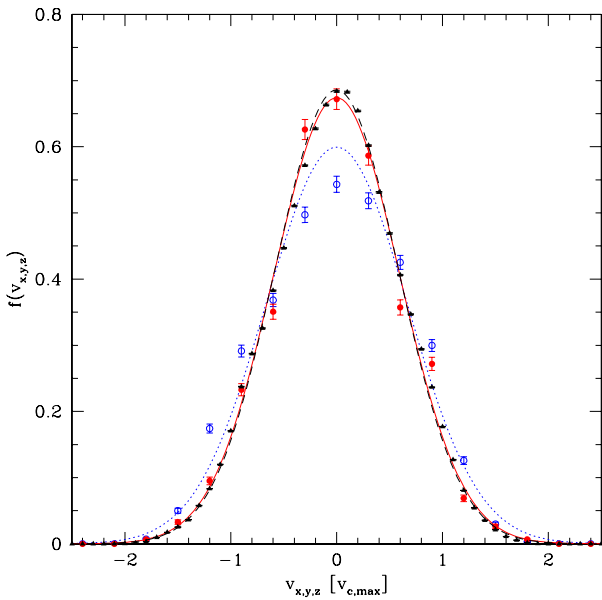


Figure 3. Velocity distributions of sample a, b and the diffuse dark matter, displayed with open squares, filled circles and triangles, respectively. The lines give the Maxwell distribution according to the mean velocity dispersion of each sample only objects in the range  $0.2 < r = r_{\text{vir}} < 1$  are used. Including also the inner  $0.2r_{\text{vir}}$  would not change this plot significantly (compare with Table 1).

$r_{[0:2;1]}$	a		b		diff	
$=v_{\text{cm, max}}$	0.665	0.007	0.5917	0.023	0.5816	0.0001
kurtosis	0.61	0.16	0.16	0.44	0.241	0.003
	0.073	0.031	0.17	0.11	0.1103	0.0005
N	4115		339		10.9	$10^6$
$r_{[0:1]}$	a		b		diff	
$=v_{\text{cm, max}}$	0.675	0.007	0.612	0.023	0.6037	0.0001
kurtosis	0.55	0.15	0.08	0.43	0.130	0.003
	0.064	0.030	0.19	0.10	0.136	0.0005
N	4239		367		14.0	$10^6$

Table 1. Velocity dispersion, kurtosis ( $v^4 = \langle v^4 \rangle - 3$ ) and anisotropy parameter  $\beta = 1 - 0.5 \frac{\langle v_r^2 \rangle - \langle v_\theta^2 \rangle}{\langle v_\theta^2 \rangle}$  of the sub-halo sample (a), the galaxy sample (b) and the diffuse dark matter (diff). Including objects with  $0.2 < r = r_{\text{vir}} < 1$  like in Figure 3 (top,  $r_{[0:2;1]}$ ) and including all objects within the virial radius (bottom,  $r_{[0:1]}$ ).

sample and the diffuse component. On the other hand Figure 2 clearly indicates a velocity bias between the diffuse component (dashed line) and sample a. The application of a rigid lower mass limit to the present substructures does not admit the perception of these subhalos to be indestructible, as it was the case for the galaxy sample. This selection more likely discards earlier accreted, and therefore slower moving, subhalos, because they spend longer time in the tidal field of the host. This mechanism shifts the average velocity of the remaining subhalos in the sample towards higher values and causes the positive velocity bias (see Ghigna et al. 2000; Colín et al. 2000; Diem and et al. 2004). Figure 3 compares the projected velocity distributions of

the two subhalo samples and the diffuse component. The dotted, solid and dashed lines are the Maxwell distributions derived from the dispersions of the respective components. Table 1 displays the actual values of the velocity dispersions in units of the maximum circular velocity of the host halo ( $v_{\text{cm, max}} = 958 \text{ km s}^{-1}$ ). The distributions of the galaxy sample and the diffuse dark matter are very similar. The velocity dispersions (and kurtosis) of these two samples agree within the one uncertainty. The velocity dispersion of sample a, however, exceeds the two others by 15%. The corresponding velocity distribution (open triangles, Figure 3) is at-topped and not well approximated by a Maxwell distribution (dotted line). There is a lack of slow moving subhalos and a slight excess of high velocity subhalos causing a negative kurtosis of about -0.6. These features can naturally be explained by the loss of earlier accreted, slow moving, subhalos due to tidal truncation. In this context, loss means decline in particle numbers below the resolution limit of 10 particles.

The shapes of observed galaxy velocity distributions in relaxed clusters can in principle be used to infer if they follow a biased, at-topped or unbiased, Gaussian distribution. In practice this is difficult measurements since large numbers of galaxies and careful removal of interlopers are needed to achieve a significant result. There are some first hints for at-topped velocity distributions: van der Marel et al. (2000) report a negative  $h_4 = -0.024 \pm 0.005$  (which is comparable to the subhalo samples, see Diem and et al. 2004) after stacking 16 CNOCl clusters and excluding the cD galaxies. Lokas et al. (2005) found negative kurtosis values (around 0.4) in 5 out of 6 nearby relaxed Abell clusters. However, the deviations from a Gaussian are only about 1% for these 5 individual systems. Our study suggests that a kurtosis which is significantly more negative than the one for the diffuse component (which has  $k = 0.15$ ) could be an indicator for positive velocity bias (and a related spatial anisotropy). It must not necessarily be related to tangential orbits (negative  $\beta$ ) as often assumed (see e.g. van der Marel et al. 2000 and refs. therein).

The orbital anisotropy of the galaxy sample is not significantly different from the dark matter background, both are slightly radial in cluster D 12. Sample a on the other hand shows marginally tangential orbits. Note that there is significant variation from halo to halo in the  $\beta$  profiles. The average over six relaxed clusters similar to D 12 shows that the dark matter  $\beta$  grows from zero (i.e. isotropic) to about 0.35 near the virial radius and total subhalo populations (corresponding to our sample a) show a similar behaviour with a weak tendency to be closer to isotropic on average (Diem and et al. 2004).

#### 4 SUPERSONIC MOTIONS OF GALAXIES IN CLUSTERS

In the previous section it has been shown, that the velocity dispersion of the galaxy sample (sample b) and the diffuse dark matter component are very similar, contrary to the obvious bias of sample a. Observationally there exist strong indications, that at least some of the galaxies in clusters move supersonically. In this section we compute the fraction of supersonic moving galaxies and the diffuse matter

can be approximated by Maxwell velocity distributions of equal temperatures, which has been shown to be adequate by the analysis in the last section. To actually compute the Mach numbers one has to translate the velocity dispersion of the diffuse dark matter into a temperature or, equivalently, a sound speed of the ICM.

At first it will be shown here that the temperatures derived from X-ray observations of clusters are in good agreement with the velocity dispersion measured for the diffuse dark matter component. Equation 2 in Vikhlinin et al. (2005) gives a linear expression for the temperature profile measured from a sample of 13 nearby by the Chandra telescope, relaxed galaxy clusters. To apply this equation we have to find the integrated emission-weighted temperature  $hT$  for our the N-body cluster. For this purpose we use Equation 9 in Evrard et al. (1996) (see also Eq. 2 in Vikhlinin et al. 2005), which relates  $r_{180}$  to  $hT$ ,  $r_{180}$  is the radius within which the mean overdensity is 180 times the critical density. Subsequently the radial temperature profile is transformed into a velocity dispersion profile using  $\frac{1}{2} = 3k_b T = (m_p)$ ,  $k_b$  is Boltzmann's constant and  $(m_p)$  is the mean molecular weight of the gas, here we assume  $= 0.61$ . After these changes Equation 2 in Vikhlinin et al. (2005) can be written in the following way.

$$\frac{v_{\text{gas}}^2(r)}{h^2} = 1.22 h^2 i - 0.9 h^2 i \quad r=r_{\text{vir}} \quad (1)$$

Here,  $h^2 i$  is the velocity dispersion which corresponds to  $hT$  and the radius is scaled by the virial radius not like Equation 2 in Vikhlinin et al. (2005) by  $r_{180}$ . The resulting velocity dispersion profile is displayed as solid line in Fig. 2 for the radial scope given by Vikhlinin et al. (2005). The good agreement between the diffuse dark matter and the gas temperature is somewhat surprising. Only if there are no other heating sources than gravity and no radiative cooling, this behaviour is expected. However, for example the entropy profiles of clusters of galaxies indicate that the gas is heated by some additional source (e.g. Finkenauer et al. 2003; Börgni et al. 2005). Furthermore, some of the kinetic energy of the gas is expected to be deposited as turbulent motion (e.g. Schuecker et al. 2004; Faltenbacher et al. 2005). All these effects, if ever effective in the considered case, seem to balance in such a way that the observed temperature profiles are in good agreement with the velocity dispersion of the diffuse dark matter component. For the purposes pursued here the details of this balancing process are not of interest, it is sufficient to notice that velocity dispersion of the diffuse dark matter resembles the temperature of the ICM.

Under the assumption of Maxwellianity the average Mach number and the fraction of galaxies moving with Mach numbers higher than a certain value can analytically be derived. The velocity dispersion of a system of  $N$  particles is defined as the root mean square of the particles' velocities  $v_i$  (relative to the centre of mass velocity). Under the assumption of isotropy (see e.g. Lokas & Mamon 2003; Katgert et al. 2004 for a discussion of isotropy of galaxy orbits in clusters) have shown that the velocity dispersion can be related to a temperature (e.g. Binney & Tremaine 1987).

$$\frac{v^2}{N} = \frac{1}{N} \sum_i v_i^2 = \frac{3k_b T}{m} \quad (2)$$

M	1	M	2	M	3
64.44 %	8.33 %	0.18 %			

Table 2. The percentage of galaxies which are expected to have Mach numbers larger than indicated by the head line, for a temperature of the intra cluster medium which corresponds to the galaxy velocity dispersion.

where  $k_b$  is the Boltzmann factor and  $m$  is the particle mass. Thus the Maxwell distribution of the particles can then be written as

$$f(v) = N \frac{2^{-\frac{1}{2}}}{\pi^{\frac{3}{2}}} v^2 \exp\left(-\frac{1}{2} \frac{3}{m} v^2\right) \quad : \quad (3)$$

The maximum of the distribution function  $f(v)$  is located at  $v_w = \sqrt{\frac{m}{2}} = \sqrt{3}$  which corresponds to the most likely velocity. The mean velocity of this distribution expressed in terms of  $v_w$  is given by

$$v = \frac{1}{N} \int_0^{\infty} v f(v) dv = \frac{2}{\pi} v_w : \quad (4)$$

For a given temperature  $T$  which is associated with a velocity dispersion as given in Eq. 2 the adiabatic sound speed is

$$v_s = \sqrt{\frac{k_b T}{m}} = \sqrt{\frac{r}{3}} ; \quad (5)$$

where is the adiabatic constant, here we use the values for ideal gas ( $= 5/3$ ). Replacing  $v_w$  with  $\sqrt{\frac{m}{2}}$  in Equation 4 and subsequent division of the Equations 4 and 5 implies an average Mach number of

$$M = \frac{v}{v_s} = \frac{8}{\pi} = 1.24 : \quad (6)$$

Therefore, the particles of a (relaxed) N-body system which can be described by a Maxwell velocity distribution move on average with slightly supersonic velocities, if the temperature of (the gas within) the system is equivalent to the velocity dispersion of the particles. Furthermore, by integration of the Maxwell distribution the fraction of particles can be derived which are moving with Mach numbers above a certain value. Table 2 displays the fraction of particles which have Mach numbers higher than 1, 2 and 3, respectively. The results in Table 2 are derived for any set of particles which follows a Maxwell velocity distribution and where the concept of sound speed is applicable. The purpose of presenting the analysis here is to show that a high fraction, namely 64.44%, of cluster galaxies move supersonically, if the ICM has the same temperature as the galaxy sample, without the requirement for recently accreted, fast moving galaxies, which are not virialised yet.

## 5 SUMMARY AND DISCUSSION

Using a cold dark matter simulation of a cluster sized  $(3.1 \cdot 10^{14} M_{\odot})$  at  $z = 0$ ) host halo we show that the recipe of subhalo selection strongly affects the obtained velocity distribution. The subhalo selection usually applied for investigations of the velocity bias does very likely not resemble the real galaxy distribution in groups and clusters. We have generated two different subhalo samples. Sample a contains all

presently found subhalos with masses above  $2.2 \times 10^8 M_{\odot}$  (10 particles). Sample b comprises the halos, which were able to accumulate more than 200 particles before entering the host halo. The selection of sample a results in a spatial distribution of subhalos which does not resemble observed galaxy distributions in clusters. On the contrary sample b shows a number density profile which is very similar to those observed in groups and clusters (see Kravtsov et al. 2004; Nagai & Kravtsov 2005). The velocity distributions of the galaxy-sample (sample b) and the diffuse dark matter component are very similar, both components closely follow a Maxwell velocity distribution with nearly equal temperatures. The velocity dispersion of the diffuse dark matter component can be translated into a temperature and consequently into a sound speed. Under the assumption that this sound speed equals the sound speed of the ICM, which here has been justified by comparison with recent X-ray observations, the fraction of galaxies which are moving supersonically can be derived. Our main results are:

1) In agreement with other authors, we find an enhancement of the velocity dispersion in the range from 15% to 30% if sample a is compared to the diffuse dark matter component.

A basic difference between a simulation particle and subhalo, selected by current mass, is that the sub-halo can fall below the mass limit in one of the subsequent time steps, it is destructible. On average sample a comprises more recently accreted, fast moving, sub-halos since the early accreted, somewhat more slowly moving, halos are prone to destruction. The positive velocity bias in sample a results from a lack of slow moving sub-halos, i.e. a flat topped non Gaussian velocity distribution with negative kurtosis  $k = -0.6$ .

2) We find no significant velocity bias between sample b and the diffuse component. Both have nearly Gaussian velocity distributions ( $k = -0.15$ ) and small radial anisotropy ( $\sim 0.15$ ). Because sample b closely reflects the spatial distributions of galaxies within clusters we conclude that the cluster galaxies should have very similar velocity distribution as the underlying dark matter. This result supports the usual assumption of no spatial or velocity bias made when galaxy kinematics are used to estimate cluster masses (e.g. Lokas et al. 2005).

3) The difference between sample a and b lies in the persistence of their subhalos. As a consequence of the shape of the sub-halo mass distribution most of the sub-halos of sample a belong to the low mass tail of that distribution. If they lose only a small fraction of their current mass (few simulation particles) due to tidal forces, they will be dismissed from the sample. They are easy to destroy. Contrary, the members of sample b have to lose at least 95% of their mass until they are discarded. These subhalos are hard to destroy. Likewise, massive galaxies in clusters are assumed to survive for long times after accretion. This explains the good agreement of the properties of sample b with luminous galaxies in clusters. However, this picture may change when fossil groups are considered. These groups are presumably old (D'Onghia et al. 2005) and may have turned a substantial fraction of their old, slow moving, satellite galaxies into diffuse intra-group light (Da Rocha & Mendes de Oliveira 2005; Faltenbacher & Mathews 2005). Therefore, we expect the spatial and velocity distributions of fossil groups to show similar features (attenuated central number-density profile and a lack of slow moving galaxies) like found in sample

a, because destruction is efficient.

4) We find an average Mach number of 1.24 for galaxies moving within a potential well of a cluster. 65% of the galaxies move supersonically and 8% show Mach numbers larger than 2. Therefore, the recent X-ray detections of supersonic motions of the galaxies in dense environments (e.g. Sun et al. 2005; Machacek et al. 2005) do not necessarily point towards highly disturbed host systems. Faltenbacher et al. (2005) analysing a combined sample of 8 groups and clusters generated by hydrodynamical simulations including cooling and star formation (see Kravtsov et al. 1997; Kravtsov 1999; Kravtsov et al. 2002) found an average Mach number of

1.4 which is somewhat higher than the value we present here. But, they also detected a positive velocity bias of

10% which may indicate that some early accreted, slow moving galaxies were lost because of tidal stripping or merging with the central massive galaxy. In any case, a relatively high fraction of supersonically moving galaxies is a natural outcome of a relaxed Maxwellian system in equilibrium. Supersonic motions do not necessarily have to be explained by arrivals, which are not yet dynamically adjusted to the host system.

#### ACKNOWLEDGEMENTS

We are grateful to William G. Mathews for insightful comments on the draft of this paper. AF has been supported by NSF grant AST 00-98351 and NASA grant NAG 5-13275 and JD by the Swiss National Science Foundation for which we are very thankful.

#### REFERENCES

Adamic C., Biviano A., Durret F., Mazure A., 2005, A & A, 443, 17  
 Binney J., Tremaine S., 1987, Galactic dynamics. Princeton, NJ, Princeton University Press, 1987, 747p.  
 Borgani S., Finoguenov A., Kay S. T., Ponman T. J., Springel V., Tozzi P., Voit G. M., 2005, MNRAS, 361, 233  
 Caldwell N., 1987, AJ, 94, 1116  
 Chincarini G., Rood H. J., 1971, ApJ, 168, 321  
 Chincarini G., Rood H. J., 1977, ApJ, 214, 351  
 Colijn P., Klypin A. A., Kravtsov A. V., 2000, ApJ, 539, 561  
 Colless M., Dunn A. M., 1996, ApJ, 458, 435  
 Cortese L., Cavazza G., Boselli A., Iglesias-Paramo J., Carrasco L., 2004, A & A, 425, 429  
 Da Rocha C., Mendes de Oliveira C. L., 2005, MNRAS, 364, 1069  
 Diemand J., Madau P., Moore B., 2005, MNRAS, 364, 367  
 Diemand J., Moore B., Stadel J., 2004, MNRAS, 352, 535  
 D'Onghia E., Sommariva Larsen J., Romero A. D., Burkert A., Pedersen K., Portinari L., Rasmussen J., 2005, ApJ, 630, L109  
 Evrard A. E., Metzler C. A., Navarro J. F., 1996, ApJ, 469, 494  
 Faltenbacher A., Kravtsov A. V., Nagai D., Gottlöber S., 2005, MNRAS, 358, 139  
 Faltenbacher A., Mathews W. G., 2005, MNRAS, 362, 498

F inoguénov A., B organi S., T omatore L., B ohringer H., 2003, *A & A*, 398, L35

G ao L., D e Lucia G., W hite S. D. M., J enkins A., 2004, *MNRAS*, 352, L1

G higna S., M oore B., G overmato F., L ake G., Q uinn T., S tadel J., 2000, *ApJ*, 544, 616

G irardi M., D em arco R., R osati P., B organi S., 2005, *A & A*, 442, 29

H alliday C., M ilvang-Jensen B., P oirier S., P oggianti B. M., J ablonka P., A ragon-Salama nca A., S aglia R. P., D e Lucia G., P ello R., S imard L., C lowe D. I., R udnick G., D alcan ton J. J., W hite S. D. M., Z aritsky D., 2004, *A & A*, 427, 397

K atgert P., B iviano A., M azure A., 2004, *ApJ*, 600, 657

K em pner J. C., D avid L. P., 2004, *MNRAS*, 349, 385

K ravtsov A. V., 1999, Ph.D. thesis, N ew M exico State U niversity

K ravtsov A. V., G nedin O. Y., K lypin A. A., 2004, *ApJ*, 609, 482

K ravtsov A. V., K lypin A., H oman Y., 2002, *ApJ*, 571, 563

K ravtsov A. V., K lypin A. A., K hokhlov A. M., 1997, *ApJS*, 111, 73

L okas E. L., M amon G. A., 2003, *MNRAS*, 343, 401

L okas E. L., W ojtak R., G ottloeber S., M amon G. A., P rada F., 2005, *A&RXiv* A strophysics e-prints

M accio' A. V., M oore B., S tadel J., D em and J., 2005, *A&RXiv* A strophysics e-prints

M achacek M., D osaj A., F orman W., J ones C., M arkevitch M., V ikhlinin A., W arm ash A., K raft R., 2005, *ApJ*, 621, 663

M achacek M. E., N ulsen P., S tribat L., J ones C., F orman W. R., 2005, *ApJ*, 630, 280

M endes de O liveira C. L., C ypriano E. S., S odré L. J., 2006, *AJ*, 131, 158

N aga iD., K ravtsov A. V., 2005, *ApJ*, 618, 557

N eumann D. M., A maud M., G astaud R., A ghanim N., L umb D., B riel U. G., V estrand W. T., S tewart G. C., M olendi S., M ittaz J. P. D., 2001, *A & A*, 365, L74

N eumann D. M., L umb D. H., P ratt G. W., B riel U. G., 2003, *A & A*, 400, 811

S chuecker P., F inoguénov A., M iniati F., B ohringer H., B riel U. G., 2004, *A & A*, 426, 387

S omm er-Larsen J., R om eo A. D., P ortinari L., 2005, *M on. Not. R oy. A stron. Soc.*, 357, 478

S pringel V., W hite S. D. M., T ormen G., K au mann G., 2001, *MNRAS*, 328, 726

S un M., J erius D., J ones C., 2005, *ApJ*, 633, 165

S un M., V ikhlinin A., F orman W., J ones C., M urray S. S., 2005, *ApJ*, 619, 169

v an der M arel R. P., M agorrian J., C arlberg R. G., Y ee H. K. C., E llingson E., 2000, *AJ*, 119, 2038

V ikhlinin A., M arkevitch M., F orman W., J ones C., 2001, *ApJ*, 555, L87

V ikhlinin A., M arkevitch M., M urray S. S., J ones C., F orman W., V an Speybroeck L., 2005, *ApJ*, 628, 655

Y am asaki N. Y., O hashi T., F unusho T., 2002, *ApJ*, 578, 833

Z entner A. R., B erlind A. A., B ullock J. S., K ravtsov A. V., W echsler R. H., 2005, *ApJ*, 624, 505